A Grid Connected Flicker Compensation of DFIG For Power Quality Improvement

P.V Vijay Kumar
PG student
Power Systems Engineering, Department of EEE
V.S.B. Engineering College, Karur-639 111, India.

R Sakthivel
Assistant Professor
Department of EEE
V.S.B. Engineering College, Karur-639 111, India.

Abstract

For the rotor side converter (RSC) of doubly fed induction generators (DFIGs) a novel terminology called combined vector and direct power control (CVDPC) is considered. The control system is resultant of a direct current control through proper voltage vectors selection from a switching table. In reality, the proposed CVDPC has the advantage of vector control (VC) and direct power control (DPC) in a compressed control system. Its advantage in contrast with VC consists of quick dynamic outcomes, toughness besides the machine factors modification, reduced computation and minimal realization. Alternatively it includes serves in relation to DPC, with fewer harmonic alteration as well as decreased power fluctuation. A vast simulation analysis by means of MATLAB/Simulink is performed on a 9-MW wind plant made of six 1.5 MW DFIG basis wind turbines. The operation of the proposed CVDPC technique is compared through both VC and DPC during steady-state and transient state. Simulation outcomes verify the dominance of the CVDPC over both VC and DPC.

Keywords: DFIG, RSC, DPC, CVDPC.

I. INTRODUCTION

In earlier days, an enormous rise in electrical power requirement and also reduction of natural resources has ended in ecological and power crises. These have guided to an enlarged requirement for manufacture of power from renewable supply with the intention that the planet wind energy manufacture has developed considerably owing to purity and renewability. Wind energy production is likely to be 10% of the world's overall electricity before the year 2020 and is projected to be twice or more by the year 2040 [1]. Wind turbines (WTs), which act a main part within wind energy are mainly separated into fixed and variable speed technologies.

Variable speed WTs have been gradually used recently as a result of numerous benefits associated with the fixed speed technologies together with increased power capture, reduced mechanical pressures forced on the turbine, enhanced power quality and reduced acoustical noise [2]. The variable speed technologies can be subdivided into two forms such as synchronous generators including full-scale converters and doubly fed induction generators (DFIGs) including partial-scale converters. The DFIG is mainly utilized for excessive power purposes as a result of the reduced converters price and lesser power losses. The DFIG control consist of both rotor side converter (RSC) as well as grid side converter (GSC) controllers with the intention that the RSC controls stator active and reactive powers and the GSC controls dc link voltage and produces an self-sufficient reactive power specifically inserted into the grid [3].

Vector control (VC) is the largely widespread process utilized within the DFIG-based WTs [4], [5]. Several benefits are specific steady state operation, fewer power ripple and inferior converter switching frequency. Nevertheless it has certain drawbacks for instance its belief on the machine factors modification because of the decoupling terms and excessive online calculation due to the pulse width modulation (PWM) process. Additionally, the coefficients of proportional integral (PI) controllers in the conventional VC must be optimally adjusted to make sure the system stability inside the entire working limit and achieve adequate dynamic response in the transient environments [6]. This will depreciate the transient operation of VC and influence the system stability in varying process environments. To overwhelm the above mentioned troubles numerous nonlinear control techniques for instance direct torque control/direct power control (DTC/DPC) included in proposed [7], [8]. The major befits of DTC/DPC techniques comprise quick dynamic response, strength against the machine factor changes, decrease in calculation and easy realization. But they have certain drawbacks with major torque-power ripples because of excessive bandwidth of the hysteresis controllers, changeable switching frequency of converters and decline of the controller functioning in the machine opening and depleted speed procedure. While numerous adapted processes have been offered to conquer these troubles [9]–[11], their disadvantage is difficult online computation.

So as to have the advantages of VC and DTC, the combined VC and DTC (CVDPC) method has been employed effectively towards induction motor [12]–[14] and stable magnet synchronous motors [15], [16]. Nevertheless the CVDPC process has not been considered properly for the DFIG. Here it is attentive on divergence of VC and DPC by glance for relationship among their principles and exploring for an elemental general source. From this general source, to have the advantages of VC and DPC and to prevent certain of the realization problems of both of two processes, the CVDPC technique is proposed used for RSC of the DFIG. The proposed CVDPC contain numerous befits in divergence with VC, together with quick dynamic response, toughness besides the

machine factor modifications, lesser calculation and minimal realization. Alternatively it has advantages in contrast with DPC including fewer harmonic alteration and inferior power ripple. This paper is arranged as follows. Within Section II the VC and DPC techniques are explained and the general source of them is examined. Inside Section III the improved control system and its essential concepts are said. Into Section IV simulation outcomes are revealed and at last in Section V, the conclusion is offered.

II. COMBINED VECTOR AND DIRECT POWER CONTROL

A. Vector Control

VC is the highly accepted technique exploited with in the DFIG built WTs. With in this technique, the stator active and reactive powers are monitored in the rotor current VC. The current vector is decayed into the sections of the stator active as well as reactive power in synchronous reference frame. This decouples the active power control from the reactive power control. The stator active and reactive power references are determined by the maximum power point tracking (MPPT) strategy and the grid requirements, respectively. The phase angle of the stator flux space vector is usually used for the controller synchronization. However, if the stator flux oriented frame (SFOF) is used, the overall performance of VC will be highly dependent on the accurate estimation of the stator flux position. This can be a critical problem under the distorted supply voltage condition or varying machine parameters. Therefore, in this paper, the stator-voltage-oriented frame (SVOF) is used for the controller synchronization. In order to extract the synchronization signal from the stator voltage signal, a simple phase-locked-loop (PLL) system is used. The stator active and reactive powers are expressed as [3]

$$P_s=\frac{3}{2}R_e(V_s i_s\ ^*) =\frac{3}{2}(V_{ds}i_{ds}+V_{qs}i_{qs}) \quad (1)$$

$$Q_s=\frac{3}{2}\mathrm{Im}(V_s i_s\ ^*) = \frac{3}{2}(V_{qs}i_{qs} - V_{ds}i_{ds}) \quad (2)$$

As the SVOF is used for the controller's synchronization, V_{qs} vanishes and the stator active and reactive power equations are simplified to

$$P_s = \frac{3}{2}V_{ds}i_{ds} \quad (3)$$

$$Q_s = \frac{-3}{2}V_{ds}i_{ds} \quad (4)$$

According to the stator flux equations in the synchronous frame [3], in this condition, the stator currents can be written as

$$i_{ds}= \frac{-L_m}{L_s}\mathrm{i_{dr}} \quad (5)$$

$$\mathrm{i_{ds}}= \frac{-\mathrm{Lm}}{\mathrm{LS}}(\mathrm{i_{qr}} + \frac{\mathrm{Vds}}{\omega \mathrm{SLm}}) \quad (6)$$

Substituting (5) and (6) into (3) and (4) yields

$$\mathrm{P_s} =\frac{-3\mathrm{Lm}}{2\mathrm{LS}}\mathrm{V_{ds}i_{dr}} \quad (7)$$

$$\mathrm{Q_s} = \frac{3\mathrm{Lm}}{2\mathrm{LS}}\mathrm{V_{ds}}(\mathrm{i_{qr}}+ \frac{\mathrm{VdS}}{\omega \mathrm{SLM}}) \quad (8)$$

Hence through i_{dr} and i_{qr} the stator active and reactive powers are controlled correspondingly. Fig. 1 illustrates RSC based VC block diagram.

B. Direct Power Control

In the DPC method, the current control loop is eliminated and the stator active and reactive powers are controlled right away. The principles of DPC can be explained by the subsequent stator active and reactive power equations [7].

$$\mathrm{Ps} =\frac{-3\mathrm{Lm}\omega \mathrm{s}}{2\sigma \mathrm{LsLr}}|\varphi \mathrm{S}||\varphi \mathrm{r}|\mathrm{Sin}\delta \quad (9)$$

$$\mathrm{Qs} =\frac{3\omega \mathrm{S}}{2\sigma \mathrm{Ls}}|\varphi \mathrm{S}|[|\varphi \mathrm{S}| - \frac{\mathrm{Lm}}{\mathrm{Lr}}|\varphi \mathrm{r}|\mathrm{Cos}\delta] \quad (10)$$

By assuming constant magnitude for the stator and rotor flux, the derivative of (9) can be represented around as

$$\frac{\mathrm{dPs}}{\mathrm{dt}}=\frac{-3\mathrm{Lm}\omega \mathrm{s}}{2\sigma \mathrm{LsLr}}|\varphi \mathrm{S}||\varphi \mathrm{r}|\frac{d\delta}{dt}\mathrm{Cos}\delta \quad (11)$$

Equation (11) shows that the stator active power dynamics depends on the variation ofδ. Therefore, the fast active power control can be achieved by rapidly changingδ. By assuming constant magnitude for the stator flux andδ, the derivative of (10) can be represented approximately as

$$\frac{\mathrm{dQs}}{\mathrm{dt}}=\frac{-3\mathrm{Lm}\omega \mathrm{s}}{2\sigma \mathrm{LsLr}}|\varphi \mathrm{s}|\frac{\mathrm{d}|\varphi \mathrm{r}|}{\mathrm{dt}}\mathrm{Cos}\delta \quad (12)$$

Equation (12) shows that the stator reactive power dynamics depend on the rotor flux magnitude variation. Therefore, the fast reactive power control can be achieved by rapidly changing the rotor flux magnitude. The variation in the rotor flux can be carried out by applying the appropriate inverter voltage vectors to the rotor windings to rotate the rotor flux linkage vector. The rotor voltage equation can be represented and approximated in a short gap of Δt as

$$\frac{d\varphi r}{dt} = Vr - Rr\ ir \approx Vr \Rightarrow \Delta\varphi r = Vr \cdot \Delta t \quad (13)$$

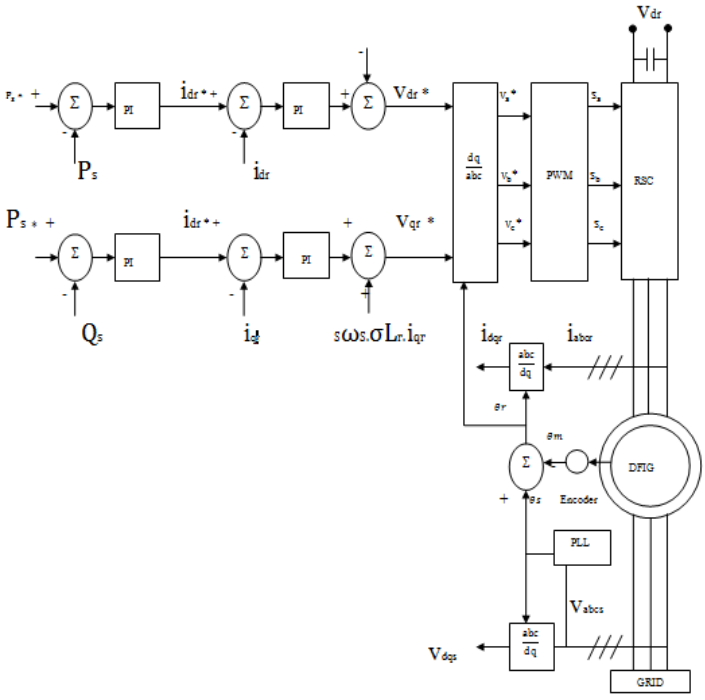

$$S\omega S.\,\sigma Lr.\,iqr - S.\frac{Lm}{Ls}.Vds$$

The six inverter voltage vectors can be correctly worn to organize the location and worth of the rotor flux φr by meaningful the division in which φr is placed.

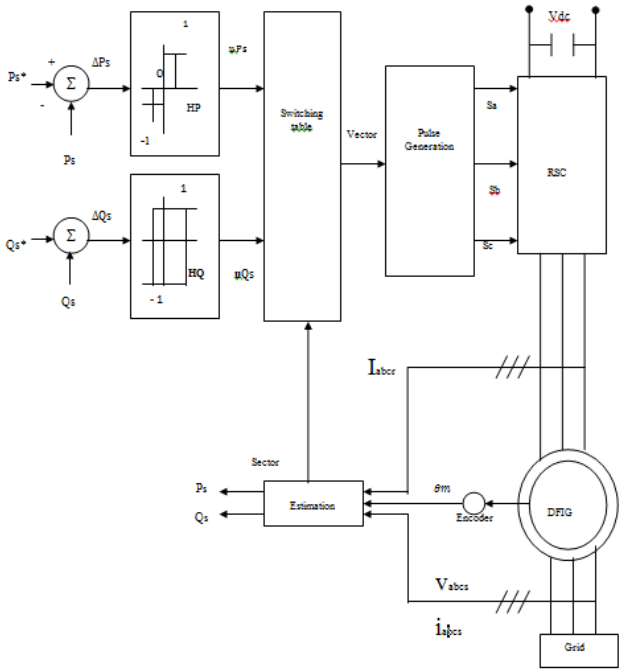

Fig. 2: Block Diagram of The Through Power Controlled RSC

Table - 1
Switching Table of Rotor Voltage Vector In DPC Method

uQs	*uPs*	*Sector*					
		1	*2*	*3*	*4*	*5*	*6*
1	*1*	*V3*	*V4*	*V5*	*V6*	*V1*	*V2*
	0	*V0*	*V7*	*V0*	*V7*	*V0*	*V7*
	-1	*V5*	*V6*	*V1*	*V2*	*V3*	*V4*
-1	*1*	*V2*	*V3*	*V4*	*V5*	*V6*	*V1*
	0	*V7*	*V0*	*V7*	*V0*	*V7*	*V0*
	-1	*V6*	*V1*	*V2*	*V3*	*V4*	*V5*

The block diagram of the through power controlled RSC is shown in Fig. 2. The hysteresis controllers generate flags (uPs and uQs) via the stator active and reactive power errors to select the greatest voltage vector from the switching table on hand in Table I [3].

C. Mathematical Similarities between VC and DPC

In this part, the numerical similarity among the VC and DPC are accessible to verify that these methods have a general base even with their performance is difference.

In the VC technique, at stable stator voltage, (7) & (8) involve that

$$\begin{cases} \text{Ps} = \frac{-3\text{Lm}}{2\text{LS}}\text{Vdsidr} \\ \text{Qs} = \frac{+3\text{LM}}{2\text{LS}}\text{Vds}(\text{iqr} + \frac{\text{Vds}}{\omega\text{SLm}}) \end{cases} \Rightarrow \begin{cases} \Delta\text{Ps}\ \alpha - \Delta\text{idr} \\ \Delta\text{Qs}\alpha\ \Delta\text{idr} \end{cases} \quad (14)$$

On top of the additional supply, allowing for the values of DPC, Fig. 3 shows the going round of the rotor flux vector φr to φr1 in an inverter switching stage, while φs remnants integral at the stator time invariable which is much longer than the inverter switching stage. Here, $\Delta\varphi$r is decomposed into its radial section $\Delta\varphi$F and its peripheral section $\Delta\varphi$T, where the previous contribute to the flux magnitude and the final provide the flux angle rotation. According to Fig. 3, (9) and (10), the statoractive and reactive power variation are obtain as

$$\Delta\text{Ps} = -\text{K1}|\varphi\text{s}|[|\varphi\text{r}|\text{Sin}(\delta + \Delta\delta) - |\varphi\text{r}|\text{Sin}\delta] \quad (15)$$

$$\Delta\text{Qs} = -\text{K2K3}|\varphi\text{s}|\text{Cos}\ \delta[|\varphi\text{r}| - |\varphi\text{r}|] \quad (16)$$

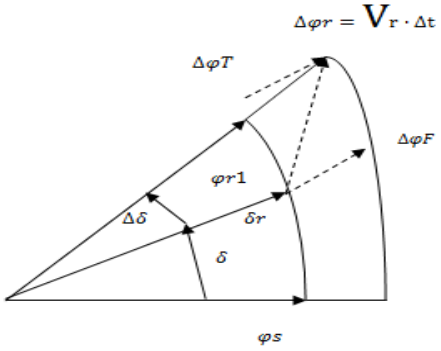

Fig. 3: Flux Linkage Vector Variation During A Switching Period In DPC

where the invariable standards of K1, K2, and K3 are known as in afterthought A. According to the little assessment of $\Delta\delta$, with a good approximation of cos $\Delta\delta$=1

$$\sin(\delta + \Delta\delta) = \text{Sin}\delta + \text{Cos}\delta \cdot \text{Sin}\Delta\delta \quad (17)$$

And $$\text{Sin}\Delta\delta = \frac{\Delta\varphi\text{T}}{|\varphi\text{r}|} \quad (18)$$

$$|\varphi\text{r1}| = |\varphi\text{r}| + \Delta\varphi\text{F} \quad (19)$$

Substituting(18) -(19)into(15)and (16)yields

$$\Delta\text{Ps} = -\text{K1}|\varphi\text{s}|\left[\Delta\varphi\text{TCos}\delta + \Delta\varphi\text{FSin}\delta + \frac{\Delta\varphi\text{T}\Delta\varphi\text{F}}{|\text{ør}|}\text{Cos}\delta\right] (20)$$

$$\Delta Qs = -K2K3|\varphi s|\Delta\varphi F\cos\delta \quad (21)$$

In (20), the second term in the collection is formed due to the partial inverter voltage vectors and inverter breakdown to part the radial and peripheral flux mechanism. This time becomes really minute by lessening the bandwidth of the hysteresis controllers. Also, the third term in the collection contain growth of small terms, such that a good estimate of the stator active power difference is obtain as

$$\Delta Ps = -K1|\varphi s|\Delta\varphi T\cos\delta \quad (22)$$

Thus

$$\Delta Ps\ \alpha\ -\Delta\varphi T \quad (23)$$

$$\Delta Qs\ \alpha\ -\Delta\varphi F \quad (24)$$

From (23) and (24), the stator active and reactive power difference are negatively comparative to the peripheral and radial machinery difference in the rotor flux in that order. By compare (23) and (24) with (14), the subsequent outcome are obtain

$$\Delta\varphi T\ \alpha\ \Delta\ idr \quad (25)$$

$$\Delta\varphi F\ \alpha\ -\Delta\ iq \quad (26)$$

It income that the variation in the peripheral and radial apparatus of the rotor flux in DPC are relative to the variation in the through and quadrature axis apparatus of the rotor current vector in VC, in that order. So, there is an apparent similarity between VC and DPC methods, so that two perpendicular variables are responsible for controlling the stator active and reactive powers separately. Certainly, two organize methods make available the same presentation if the numeral of inverter voltage vectors is not partial.

III. PROPOSED CONTROL SYSTEM

A. The Basic Idea

As exposed in Part II, there is a through connection between the hysteresis organize of the stator active power in DPC and the rotor direct axis current organize in VC. On the additional supply, it is illustrate that the hysteresis organize of the stator reactive power in DPC closely corresponds to the rotor quadrature axis current organize in VC. Due to these particulars, it is likely to suggest a new organize structure base on the general basics of equally method by combine the qualities of DPC and VC. This method, it can be potential to present a organize structure with a advantageous performance and a somewhat simpler execution. Regularly, it can be regard as a fresh structure devoid of a few of the difficulty linked with also DPC or VC.As was verified, by quicker collection of the power electronic switches position, DPC can present quicker torque/power answer. This, in order, is due to the utilize of a fixed switching table in its place of a much additional time incontrollable PWM method. Additionally, the utilize of hysteresis controller, which present input to the switching table, contribute to the quick dynamics of DPC. Then, the hysteresis controller and switching table are high quality candidate for the structure of the fresh manage structure. In the indirect VC structure, the direct axis and quadrature axis apparatus of the rotor current are controlled as a substitute of the stator active and reactive power.

B. The Control System Structure

The projected manage structure in Fig. 4 is separated keen on a VC division and a DPC division that are exposed on the left side and the right side of the figure, in that order. As seen, the structure use the d axis and q axis hysteresis current controllers comparable to those in VC and the switching table similar to the single in DPC. The d axis and q axis current orders are conservatively generated by the PI power controllers and compare with their real ideals. Of path the orientation frame conversion is necessary as in VC. The d axis and q axis paper chain as input to the switching table are shaped from the rotor current errors by the hysteresis controllers. The third inputs to the switching table determine the sector from side to side which the rotor flux vector is transitory. It is increase by measure the stator and rotor currents and the rotor location. The switching table provide the good voltage vectors by select the position of the inverter switch, the equal as in DPC. The switching table is given away from the Table I, which produce all eight voltage vectors as well as zero voltages. The structure lack PI current controllers, a PWM, and nourish pass on conditions that are regularly accessible in the VC structure. In reality, the structure is a current VC structure by funds of a voltage vector choice of the DPC nature.

IV. SIMULATION RESULTS

Here part, an widespread simulation revise, with MATLAB/Simulink, is conduct on a 9-MW wind ranch consisting of six 1.5-MW DFIG base wind turbines to match up to the presentation of the projected CVDPC process through equally VC and DPC.

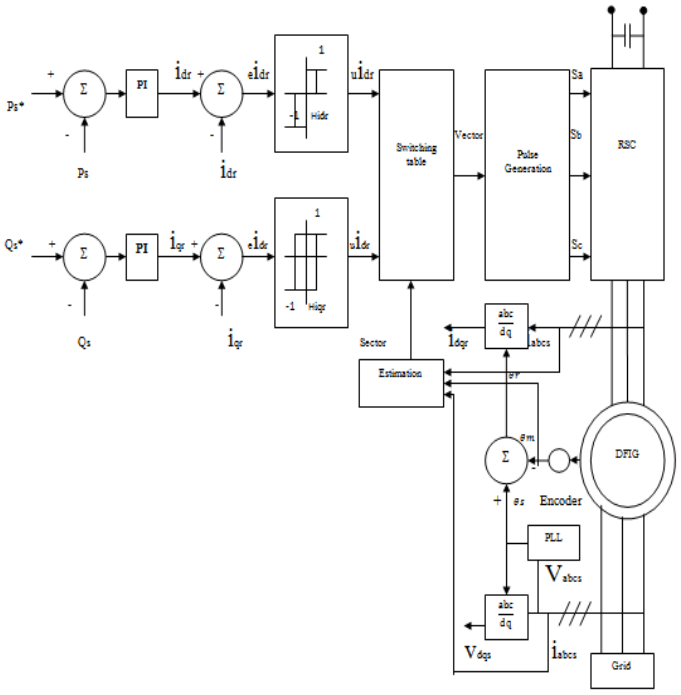

Fig. 4: Proposed Control System.

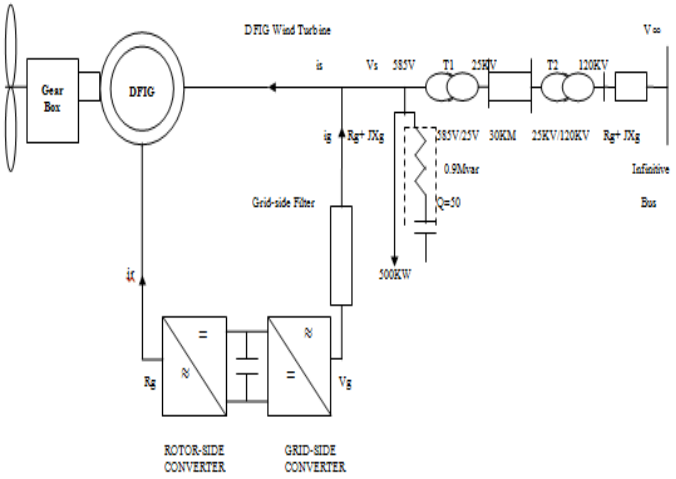

Fig. 5: Schematic Diagram of The Simulated System.

Fig. 5 show the chart diagram of the simulated structure with parameter set in After thought B. Normally, in arrange to appraise the CVDPC technique, the valuation is separated addicted to two part, the first part is connected to the steady state setting and the second part is about the passing conditions. The bandwidth of hysteresis current controller is set to $\delta = 2\Delta\delta = 0.02$ p.u. inthis study. With select these ideals, aexchange between the rotorcurrent track accurateness and the greatest switching frequency(MSF) of the RSC is obtain. An best possible alteration of the PI manager gain is needed to reach a reasonable relationship between the three method. Then, the optimal conventional controller (OCC) of the PI type is used. The controller parameter is optimized by by means of the normal optimization genetic algorithm (GA). The manage loops of the stator active and reactive powers and rotor currents contain been optimized below the stable setting of rotor speed and stator reactive power at $\omega r = 1{:}2$ p.u. and $Qs = 0$ p.u. at the same time. The cost purpose of the optimization algorithm is clear as

$$J = \int_{t1=0}^{t2} (|\Delta Ps| + |\Delta Qs|) dt \quad (27)$$

The junction of the cost purpose in every optimization step is shown in Fig. 6.

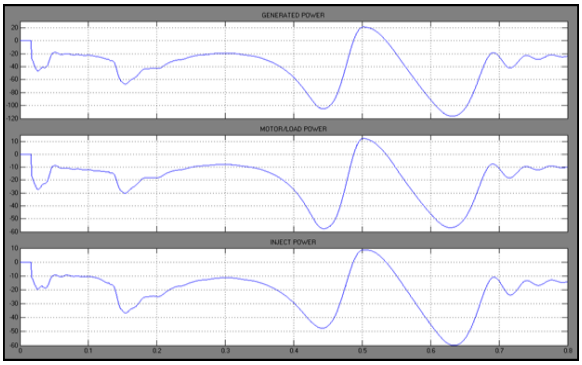

Fig. 6: Output Power Wave Form

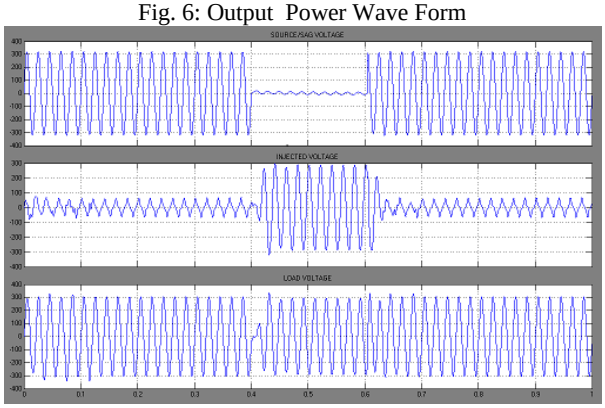

Fig. 7: Output Voltage Level

Fig. 7 shows the structure simulation output in the steady state situation for $0 < t < 0.3$ s. The unspecified steady wind speed is 15 m/s when the generators rotate at ωr=1.2 p.u. base on the simulated best possible power speed curve. As so, the active power of 9 MW is generated in the wind ranch. As the DFIGs rotate at super synchronous speed with s= -0.2, the active power is deliver to the grid from side to side stator and rotor windings (Ps = 7.58 MW and Pr =1.42 MW). According to the greatest utilize of the RSC current capacity for produce active power, the stator reactive power making is zero. Allowing for the output specified in Fig. 7, it can be completed that the CVDPC has power ripple as short as that of VC, which is equivalent to 0.55%. Also, it operates the machine considerably softer than DPC with a ripple of 2.22%.

Furthermore, the steady state presentation of the CVDPC is compare by equally VC and DPC in conditions of the harmonic distortion of the stator result current and the MSF of the RSC by a Fast Fourier transform (FFT) studies. Fig. 8 shows the stator three phase currents and harmonic spectrum. For VC, the total harmonic distortion (THD) is equivalent to 1.28% and the switching frequency particular by the carrier waveform, e.g., 2.5 kHz. As well, in case of the DPC, the THD is equivalent to 4.64%, and the MSF is imperfect to 7.5 kHz. Though, by using CVDPC, the THD of the stator current is equivalent to 2.10% and the MSF is imperfect to 7.5 kHz. So, the THD level and the amplitudes of the separate harmonic apparatus are lesser than the allowable distortion limits suggested in IEEE Standard 1547 [17]. Therefore, it can be completed that the CVDPC has a fitting THD as less important as that of VC, which is not as much of than that of DPC. The second part of the valuation includes the passing setting below the changeable wind speed. Fig. 9 shows the simulation output in these setting. Even as the wind speed step change from 15 to 10 m/s at t= 0.3 s, the rotor speed variation from 1.2 to 0.8 p.u. and the stator active power construction decrease from 7.58 to 2.81 MW. When the DFIGs turn around at sub synchronous speed with s =+0.2, 20% of the stator active power is fed back to the machine from side to side the converters (Pr=-0:6 MW). Communication that the stator active power variation are obtain by lessening Idr from 0.79 to 0.3 p.u., as Iqr is kept stable. This matter illustrate the sovereign manage of the stator active and reactive powers. Communication that through the synchronous process about t = 1.82 s, no active power is transfer from the end to end converters linked to the rotor. Allowing for the output, it can be completed that the CVDPC respond to the wind speed variation just about as quick as that of DPC, which better the VC in conditions of dynamic result.

In arrange to evaluate the projected CVDPC with VC in conditions of strength and decoupled performance, varying Rr is optional. Fig. 10 shows the simulation output in this order. So, at t =0.3 s, Rr is improved to four times the current worth. As a output, the total active power experiences the passing condition before inveterate to the steady state process. The stator active power increase from 7.58 to 8 MW and the rotor active power decrease from 1.42 to 1 MW, but the stator reactive power remnants unmovable. As it is notice in Fig. 10, when Rr is altered, the CVDPC-like DPC operate more strongly in assessment with VC.

V. CONCLUSION

Inside this paper, by considering the configuration of VC and DPC a novel collective control structure derived from the general core of both techniques has been offered designed for the RSC of the DFIG. The united system uses the present VC approach which produces the rotor current components and utilizes the DPC-based switching table. The improved CVDPC process has been

evaluated by both the VC based optimized PI controllers and DPC in conditions of minimal realization, suitable power ripples and proper dynamic response. Therefore the proposed CVDPC technique offers a cooperation of the benefits of two processes.

During the steady state situations, the CVDPC enclose power ripple as minimal as that of VC. The ripple is considerably inferior in difference with that of DPC. Besides an FFT examination illustrate that CVDPC has a appropriate THD as minimal as that of VC which is fewer than that of DPC. During the transient conditions, the CVDPC react to the wind speed changes almost as ahead as DPC which better VC in conditions of dynamic response. Furthermore the CVDPC like DPC achieves VC in offering suitable decoupling and toughness against the machine factors modification. Therefore proposed CVDPC not only have reduced power ripple as superior as VC nevertheless maintains prominent dynamic response as quick as DPC.

REFERENCES

[1] World Wind Energy Association WWEA. (2011, Apr.). World Wind Energy Report 2010, Germany [Online]. Available: http://www. WWindEA.org.
[2] M. Mohseni, S. Islam, and M. A. S. Masoum, "Enhanced hysteresis-based current regulators in vector control of DFIG wind turbines," IEEE Trans. Power Electron., vol. 26, no. 1, pp. 223–234, Jan. 2011.
[3] G. Abad, J. Lopez, M. A. Rodriguez, L. Marroyo, and G. Iwanski, Doubly Fed Induction Machine Modeling and Control for Wind Energy Generation Applications. Hoboken, NJ, USA: Wiley, 2011.
[4] H. M. Jabr, D. Lu, and N. C. Kar, "Design and implementation of neuro-fuzzy vector control for wind driven doubly fed induction generator," IEEE Trans. Sustain. Energy, vol. 2, no. 4, pp. 404–413, Oct. 2011.
[5] S. Li, T. A. Haskew, K. A. Williams, and R. P. Swatloski, "Control of DFIG wind turbine with direct-current vector control configuration," IEEE Trans. Sustain. Energy, vol. 3, no. 1, pp. 1–11, Jan. 2012.
[6] J. P. A. Vieira1, M. V. A. Nunes, U. H. Bezerra, and A. C. Nascimento, "Designing optimal controllers for doubly fed induction generators using a genetic algorithm," IET Gen. Transm. Distrib., vol. 3, no. 5, pp. 472–484, May 2009.
[7] L. Xu and P. Cartwright, "Direct active and reactive power control of DFIG for wind energy generation," IEEE Trans. Energy Convers., vol. 21, no. 3, pp. 750–758, Sep. 2006.
[8] J. Hu, H. Nian, B. Hu, and Y. He, "Direct active and reactive power regulation of DFIG using sliding-mode control approach," IEEE Trans. Energy Convers., vol. 25, no. 4, pp. 1028–1039, Dec. 2010.
[9] G. Abad, M. A. Rodriguez, and P. Poza, "Two-level VSC-based predictive direct power control of the doubly fed induction machine with reduced power ripple at low constant switching frequency," IEEE Trans. Energy Convers., vol. 23, no. 2, pp. 570–580, Jun. 2008.